

AMES-HET-98-07
MADPH-98-1052
hep-ph/9806486
June 1998

Single Top Quark Production via FCNC Couplings at Hadron Colliders

T. Han^a, M. Hosch^b, K. Whisnant^b, Bing-Lin Young^b, and X. Zhang^c

^a *Department of Physics, University of Wisconsin,
Madison, WI 53706, USA*

^b *Department of Physics and Astronomy, Iowa State University,
Ames, Iowa 50011, USA*

^c *CCAST (World Laboratory), P.O. Box 8730, Beijing 100080, and
Institute of High Energy Physics, Academia Sinica, Beijing 100039, China*

Abstract

We calculate single top-quark production at hadron colliders via the chromo-magnetic flavor-changing neutral current couplings $\bar{t}cg$ and $\bar{t}ug$. We find that the strength for the anomalous $\bar{t}cg$ ($\bar{t}ug$) coupling may be probed to $\kappa_c/\Lambda = 0.092 \text{ TeV}^{-1}$ ($\kappa_u/\Lambda = 0.026 \text{ TeV}^{-1}$) at the Tevatron with 2 fb^{-1} of data and $\kappa_c/\Lambda = 0.013 \text{ TeV}^{-1}$ ($\kappa_u/\Lambda = 0.0061 \text{ TeV}^{-1}$) at the LHC with 10 fb^{-1} of data. The two couplings may be distinguished by a comparison of the single top signal with the direct top and top decay signals for these couplings.

1 Introduction

Since the discovery of the top quark at the Fermilab Tevatron [1], there has been considerable interest in exploring the properties of the top quark. Its unusually large mass close to the electroweak symmetry-breaking scale makes it a good candidate for probing for physics beyond the Standard Model (SM) [2], and has also given rise to explorations of anomalous couplings of the top quark [3, 4, 5].

A distinctive set of anomalous interactions is given by the flavor-changing chromo-magnetic operators [6, 7]:

$$\frac{\kappa_f}{\Lambda} g_s \bar{f} \sigma^{\mu\nu} \frac{\lambda^a}{2} t G_{\mu\nu}^a + h.c. , \quad (1)$$

where Λ is the new physics scale, $f = u$ or c , the κ_f define the strength of the $\bar{t}ug$ or $\bar{t}cg$ couplings, and $G_{\mu\nu}^a$ is the gauge field tensor of the gluon. Although such interactions can be produced by higher order radiative corrections in the SM, the effect is too small to be observable [8]. Any signal indicating these types of couplings is therefore evidence of physics beyond the SM, and will shed more light on flavor physics in the top-quark sector. It has been suggested that couplings of this type may be large in some extensions to the standard model, especially in models with multiple Higgs doublets such as supersymmetry [8, 9, 10]. Models with new dynamical interactions of the top quark [11] and those in which the top quark is composite [12] or has a soliton [13] structure could also give rise to the new couplings in Eq. (1).

Currently, there only exist rather loose bounds on these anomalous couplings. The good agreement between the SM theory and experiments in top-quark production at the Fermilab Tevatron [1] places a modest limit on the couplings in Eq. (1). By looking for signals from $t \rightarrow cg$ or ug decays [6], the coupling parameters κ_f/Λ can be constrained down to 0.43 TeV^{-1} with the existing Tevatron Run 1 data.

In this paper, we examine the effect of these couplings on single top-quark production at the Tevatron and the CERN LHC. There are four different subprocesses which lead to one top quark in the final state together with one associated jet. The identity of the associated jet depends upon the initial state of the system:

$$q\bar{q} \rightarrow t\bar{c}, \quad gg \rightarrow t\bar{c}, \quad cq(\bar{q}) \rightarrow tq(\bar{q}), \quad cg \rightarrow tg. \quad (2)$$

We also consider similar processes which replace the c quark with the u quark, as well as similar processes for single anti-top quark production. The

advantage of this class of events is the unique production mechanism and the distinctive final state kinematics over the SM backgrounds.

The effect of the anomalous $\bar{t}cg$ coupling on single top quark production via the $q\bar{q}$ process in Eq. (2) at the Tevatron has been studied in Ref. [14]. It was found that κ_c/Λ can be measured to 0.4 TeV^{-1} with the existing Tevatron data, comparable to the limit obtained by the anomalous top decay processes [6] mentioned earlier. We find, however, that the other processes in Eq. (2) are also important, especially at higher energies. This is particularly true for the case of κ_u/Λ .

This paper is organized as follows. In Sec. 2, we discuss the signal and background calculations. We also study a set of acceptance cuts to optimize the signal observability. In Sec. 3, we discuss our results and related issues, and make some concluding remarks.

2 Signal and Background Calculations

We calculate the tree level cross sections for single top (or anti-top) quark production of Eq. (2) at hadron colliders using the flavor-changing chromo-magnetic couplings in Eq. (1). For completeness, we study the following collider parameters for the center-of-mass energy and integrated luminosity:

		E_{cm} (TeV)	\mathcal{L} (fb $^{-1}$)
Tevatron	Run 1	1.8	0.1
	Run 2	2	2
	Run 3	2	30
LHC		14	10

As for the final state signature, while the $t \rightarrow cg$ or ug decay will occur due to the anomalous couplings in Eq. (1), the branching ratio becomes negligible when κ_f/Λ is less than about 0.2 TeV^{-1} . For this reason, and since the top-quark decay $t \rightarrow bW \rightarrow bl\nu_\ell$ is easier to identify than the pure hadronic mode, we will choose as the search mode for the signal

$$p\bar{p} \rightarrow t + j \rightarrow bl\nu_\ell + j, \quad (3)$$

where j is a light parton jet and $\ell = e, \mu$. We assume that the top quark is on mass shell when we calculate the decay process, but the spin correlation

effects are fully incorporated. In determining the branching ratio of $t \rightarrow Wb$, we have properly included the contribution from $t \rightarrow cg$ or ug . This term is proportional to $|\kappa_f/\Lambda|^2$ and it only appreciably affects the branching ratio if $\kappa_f/\Lambda \gtrsim 0.2 \text{ TeV}^{-1}$. The calculated cross sections are shown in Fig. 1 as a function of κ_f/Λ , for the Fermilab Tevatron ($p\bar{p}$ at the center of mass energy $\sqrt{s} = 1.8 \text{ TeV}$) and for the CERN LHC (pp at $\sqrt{s} = 14 \text{ TeV}$), using the MRSA structure functions [15]. Results for the Tevatron at 2 TeV are nearly indistinguishable from the cross sections shown here for 1.8 TeV.

In order to simulate the detector effects in identifying the signal, we made a series of standard cuts on the transverse momentum p_T , the missing transverse momentum resulting from the neutrino \cancel{p}_T , pseudorapidity η , and the jet (lepton) separation ΔR . We call these the “basic cuts”:

$$p_{Tb}, p_{Tj}, p_{Tl}, \cancel{p}_T \geq 15 \text{ GeV} , \quad (4)$$

$$\eta_b, \eta_j, \eta_l \leq 2.5 , \quad (5)$$

$$\Delta R_{jj}, \Delta R_{jl} \geq 0.4 . \quad (6)$$

To be more realistic, we also assume a Gaussian smearing of the energy deposited in calorimeters, given by:

$$\Delta E/E = 30\%/\sqrt{E} \oplus 1\% , \text{ for leptons} , \quad (7)$$

$$= 80\%/\sqrt{E} \oplus 5\% , \text{ for hadrons} , \quad (8)$$

where \oplus indicates that the two terms are added in quadrature.

The major source of background to signal production in Eq. (3) is

$$p\bar{p} \rightarrow W + jj , \quad (9)$$

where the jets are light quarks or gluons. An effective way to reduce the background is to employ b -tagging. We take a b -tagging efficiency of 36% at Run 1 of the Tevatron, and 60% at Runs 2 and 3 and at the LHC. We also assume that 1% of non- b quarks would be misidentified as b quarks in all of the experiments, which gives a suppression of the $W + jj$ background by a factor of ≈ 50 . Other significant backgrounds are standard model single top quark production where one light quark accompanies the top quark in the final state [16], and standard model $Wb\bar{b}$ production. Backgrounds with two b quarks in the final state will mimic our signal if one of the b quarks is missed by the b tag.

We used the VECBOS Monte Carlo [17] to calculate the cross sections for the Wjj and $Wb\bar{b}$ backgrounds. We made two modifications to the VECBOS code. First, we added a routine to calculate some of the kinematic distributions, as described below, that we found to be very helpful for background suppression. Second, since our signal process involves one b quark in the final state, b -tagging was crucial in eliminating the Wjj background; we modified the code to randomly choose one of the jets to be mis-identified as a b -jet (with probability of 1%). For the calculation of the standard model single top processes $bq \rightarrow tq$ and $q\bar{q} \rightarrow t\bar{b}$ we used our own monte carlo routine [18].

To further enhance the signal relative to the Wjj and $Wb\bar{b}$ backgrounds, we imposed a constraint on M_{bW} , the invariant mass of the W and b quark, which should be peaked at m_t for the signal. To experimentally determine M_{bW} , one must reconstruct $p_t = p_b + p_l + p_{\nu_l}$. The neutrino is not observed, but its transverse momentum can be deduced from the missing transverse momentum. The longitudinal component of the neutrino momentum is determined by setting $M_{\nu_l} = M_W$, and is given by:

$$p_L^{\nu_l} = \frac{\chi p_L^l \pm \sqrt{\vec{p}_T^2 (\chi^2 - p_{Tl}^2 p_{T\nu_l}^2)}}{p_{Tl}^2}, \quad (10)$$

where

$$\chi = \frac{M_W^2}{2} + \vec{p}_T^l \cdot \vec{p}_T^{\nu_l}, \quad (11)$$

and p_L refers to the longitudinal momentum. Note that there is a two fold ambiguity in this determination. We chose the solution in which M_{bW} is closer to the mass of the top quark. This process artificially inserts a broad peak in the background at $M_{bW} = m_t$, but since the signal peak is much sharper, the M_{bW} distribution is still an effective variable to use to increase the signal-to-background ratio.

To find a way to further isolate the signal from the background, we examined the kinematic distributions in $\sqrt{\hat{s}}$, M_{bW} , p_T , η , and ΔR . Three of the variables, M_{bW} , p_{Tb} , and ΔR_{jj} , are especially useful for significantly suppressing the background and therefore improving the discovery limit for the κ_f/Λ . Just as M_{bW} has a peak near m_t for the signal, p_{Tb} develops its Jacobian peak near $\frac{1}{2}m_t\sqrt{1 - M_W^2/m_t^2}$. Furthermore, ΔR_{jj} reaches a peak near π for the signal since the two jets are largely back-to-back. To effectively reduce the background versus the signal we applied the additional cuts for

the Tevatron Run 1

$$150 \text{ GeV} \leq M_{bW} \leq 200 \text{ GeV}, \quad (12)$$

$$p_{Tb} \geq 35 \text{ GeV}, \quad (13)$$

$$\Delta R_{jj} \geq 1.0, \Delta R_{lj} \geq 0.4. \quad (14)$$

The distributions for these variables are shown for Run 1 in Figs. 2–5 after the cuts in Eqs. (4)–(6) and (12)–(14) are applied. For Run 2 and Run 3 and for the LHC, the signal-to-background ratio can be improved by changing the cuts in Eqs. (12)–(14). The optimized cuts for each collider option are shown in Table 1. The cross sections for the signal and background channels after all cuts are shown in Table 2.

In Ref. [14] anomalous single top quark production was studied through only one channel, $q\bar{q} \rightarrow t\bar{c}$. As Table 2 shows, this is the least important of all of the channels in Eq. (2). While it would seem that the presence of initial state valence quarks ought to make this the dominant process, the massless t -channel exchange of a gluon in the $cq \rightarrow tq$ process more than makes up for the lack of initial state valence quarks, and it becomes the most important process. Each of the other processes, $cq \rightarrow tq$ and $gg \rightarrow t\bar{c}$, also have massless, or nearly massless, t -channel exchanges which increase their parton cross sections. We also note that in Ref. [14] a cut on the center of mass energy, $\sqrt{\hat{s}} > 300 \text{ GeV}$, was imposed for the purpose of reducing the background relative to the signal. Because of the dominance of the massless t -channel exchanges, the parton cross section is peaked at lower values of $\sqrt{\hat{s}}$ when all of the processes in Eq. (2) are included. Hence, the $\sqrt{\hat{s}}$ cut is not useful in our calculation as it will reduce the signal drastically.

3 Discussion and Summary

We may use the results of the signal and background calculation to determine the minimum values of κ_c/Λ and κ_u/Λ that can be observed at hadron colliders. We use the criterion that $N_S \geq 3\sqrt{N_S + N_B}$ approximately corresponding to a 95% confidence level, where N_S and N_B are the number of signal and background events, respectively. Since the signal is quadratic in κ_f/Λ and we have calculated the signal for $\kappa_f/\Lambda = 0.2 \text{ TeV}^{-1}$, the minimum

value of κ_f/Λ is then given by

$$\frac{\kappa_f}{\Lambda} = 0.2 \text{ TeV}^{-1} \sqrt{\frac{\frac{9}{2}(1 + \sqrt{1 + \frac{4}{9}\mathcal{L}\sigma_B})}{\mathcal{L}\sigma_0}}, \quad (15)$$

where \mathcal{L} is the integrated luminosity, σ_B is the total cross section for all of the background processes, and σ_0 is the cross section for the signal processes evaluated at $\kappa_f/\Lambda = 0.2 \text{ TeV}^{-1}$. The discovery limits, calculated using the basic cuts, the optimized cuts in Table 1, and b -tagging, are shown in Table 3.

A search for direct top quark production (where the top quark is the only particle in the final state of the parton process) will also place a limit on the size of κ_f/Λ [7]. This process relies on its rare signature and on the large fraction of gluons in the initial state to boost its signal relative to the background. The up quark operator in Eq. (1) has the additional bonus that the initial state quark is a valence quark. With b -tagging (of the top quark decay products), direct top quark production provides nearly ideal conditions for measuring the anomalous coupling parameters. Using this process, κ_c/Λ (κ_u/Λ) can be measured down to $.062 \text{ TeV}^{-1}$ ($.019 \text{ TeV}^{-1}$) at Run 2 of the Tevatron with 2 fb^{-1} integrated luminosity, and to $.0084 \text{ TeV}^{-1}$ ($.0033 \text{ TeV}^{-1}$) at the LHC with 10 fb^{-1} integrated luminosity. Thus direct top production provides a second, independent measurement of these anomalous couplings.

The c and u quarks have, so far, been treated as if only one of the couplings exists at a time. If the two anomalous couplings co-exist, we may simply add the cross sections of the two different couplings together, since we have treated them in exactly the same manner. A plot of their discovery limits, when considered together, is shown in Fig. 6.

If a signal is seen, how can we determine if it is due to $\bar{t}cg$, $\bar{t}ug$, or perhaps a mixture of the two? If the c or u quark is in the final state, then charm tagging could in principle distinguish between the two couplings. However, the signal processes in which this occurs (i.e., the single top processes $q\bar{q} \rightarrow t\bar{c}, t\bar{u}$ and $gg \rightarrow t\bar{c}, t\bar{u}$, and the anomalous top decays $t \rightarrow cg, ug$) have smaller cross sections than the signal processes where the c or u quark is in the initial state (the single top processes $cq, uq \rightarrow tq$ and $gc, gu \rightarrow gt$, and the direct top processes $gc, gu \rightarrow t$). Furthermore, the efficiency for charm-quark tagging is expected to be low compared to b -quark tagging. Therefore it will be difficult to distinguish the $\bar{t}cg$ and $\bar{t}ug$ couplings with charm tagging.

Another possibility is to compare the relative size (after all the cuts and

b -tagging) of the anomalous single top cross section σ_{st} , the direct top cross section σ_{dt} [7], and the $t\bar{t}$ production cross section when the t (\bar{t}) undergoes an anomalous decay into cg ($\bar{c}g$) or ug ($\bar{u}g$), $\sigma_{at\bar{t}}$ [6]. For example, at the Tevatron Run 2 for $\kappa_c/\Lambda = 0.2 \text{ TeV}^{-1}$ these cross sections are $\sigma_{st} = 154 \text{ fb}$, $\sigma_{dt} = 281 \text{ fb}$, and $\sigma_{at\bar{t}} = 6 \text{ fb}$, while for $\kappa_u/\Lambda = 0.2 \text{ TeV}^{-1}$ they are $\sigma_{st} = 1976 \text{ fb}$, $\sigma_{dt} = 2990 \text{ fb}$, and $\sigma_{at\bar{t}} = 6 \text{ fb}$. The ratios $\sigma_{st}/\sigma_{at\bar{t}}$ and $\sigma_{dt}/\sigma_{at\bar{t}}$ are much larger for the $\bar{t}ug$ coupling than for $\bar{t}cg$. Also, σ_{st}/σ_{dt} is somewhat larger for the $\bar{t}ug$ coupling than for $\bar{t}cg$. Hence, a comparison of two or more of these signals may help determine whether the anomalous coupling is $\bar{t}cg$, $\bar{t}ug$, or a mixture of the two.

In summary, we calculated the single top–quark production at hadron colliders via the chromo–magnetic flavor–changing neutral current couplings $\bar{t}cg$ and $\bar{t}ug$. We find that the strength for the anomalous coupling $\bar{t}cg$ may be probed to $\kappa_c/\Lambda = 0.092 \text{ TeV}^{-1}$ at the Tevatron with 2 fb^{-1} of data at 2 TeV and $\kappa_c/\Lambda = 0.013 \text{ TeV}^{-1}$ at the LHC with 10 fb^{-1} of data at 14 TeV. Similarly, the anomalous coupling $\bar{t}ug$ may be probed to $\kappa_u/\Lambda = 0.026 \text{ TeV}^{-1}$ at the Tevatron and $\kappa_u/\Lambda = 0.0061 \text{ TeV}^{-1}$ at the LHC. Assuming $\kappa_c \equiv 1$ ($\kappa_u \equiv 1$), the scale of new physics Λ can be probed to 11 TeV (38 TeV) at the Tevatron and to 77 TeV (164 TeV) at the LHC.

4 Acknowledgments

This work was supported in part by the U.S. Department of Energy under Contracts DE-FG02-94ER40817 and DE-FG02-95ER40896. Further support for T.H. was provided by the University of Wisconsin Research Committee, with funds granted by the Wisconsin Alumni Research Foundation. M. Hosch was also partially supported by GAANN.

References

- [1] F. Abe et al., Phys. Rev. Lett. **74**, 2626 (1995); S. Abachi et al., Phys. Rev. Lett. **74**, 2632 (1995).
- [2] For a recent review on implications of a heavy top quark, see *i. e.*, E. H. Simmons, hep-ph/9707452; and references therein.
- [3] J. Incandela, Nuovo Cim. **109A**, 741 (1996); Thomas J. LeCompte, FERMILAB-CONF-96-021-E (Jan 1996); A.P. Heinson, FUTURE TOP PHYSICS AT THE TEVATRON AND LHC, in *Les Arcs 1996, QCD and high energy hadronic interactions* 43-52.
- [4] D. Atwood, A. Kagan and T.G. Rizzo, Phys. Rev. **D 52**, 6264 (1995); Douglas O. Carlson, Ehab Malkawi and C.P. Yuan, Phys. Lett. **B 337**, 145 (1994); G.J. Gounaris, M. Kuroda and F.M. Renard, Phys. Rev. **D 54**, 6861 (1996); G.J. Gounaris, J. Layssac, F.M. Renard, THES-TP-96-12 (Nov 1996).
- [5] T. Han, R.D. Peccei, and X. Zhang, Nucl. Phys. **B 454**, 527 (1995); T. Han, K. Whisnant, Bing-Lin Young and X. Zhang, Phys. Rev. **D 55**, 7241 (1996); K. Whisnant, Jin-Min Yang, Bing-Lin Young and X. Zhang, Phys. Rev. **D 56**, 467 (1997); R. Martinez and J-Alexis Rodriguez, Phys. Rev. **D 55**, 3212 (1997).
- [6] T. Han, K. Whisnant. Bing-Lin Young and X. Zhang, Phys. Lett. **B 385**, 311 (1996).
- [7] M. Hosch, K. Whisnant and Bing-Lin Young, Phys. Rev. **D 56**, 5725 (1997).
- [8] G. Eilam, J.L. Hewett and A. Soni, Phys. Rev. **D 44**, 1473 (1991).
- [9] B. Grzadkowski, J.F. Gunion and P. Krawczyk, Phys. Lett. **B 268**, 106 (1991); M. Luke and M.J. Savage, Phys. Lett. **B 307**, 387 (1993); G. Couture, C. Hamzaoui and H. König, Phys. Rev. **D 52**, 1713 (1995); Jorge L. Lopez, D.V. Nanopoulos and Raghavan Rangarajan, Phys. Rev. **D 56**, 3100 (1997); T. P. Cheng and M. Sher, Phys. Rev. **D 48**, 3484 (1987); W.S. Hou, Phys. Lett. **B 296**, 179 (1992); L.J. Hall and S. Weinberg, Phys. Rev. **D 48**, 979 (1993); D. Atwood, L. Reina and A. Soni, Phys. Rev. **D 53**, 1199 (1996).

- [10] Jin Min Yang, Bing-Lin Young, and X. Zhang, hep-ph/9705341.
- [11] C.T. Hill, Phys. Lett. **B 266**, 419 (1991); *ibid.* **B 345**, 483 (1995); B. Holdom, Phys Lett **B 339**, 114 (1994); *ibid.* **B 351**, 279 (1995).
- [12] H. Georgi, L. Kaplan, D. Morin and A. Schenk, Phys. Rev. **D 51**, 3888 (1995); for a review of composite models, see, e.g., R.D. Peccei in: Proc. 1987 Lake Louise Winter Institute: Selected Topics in the Electroweak Interactions, eds. J.M. Cameron et al. (World Scientific, Singapore, 1987).
- [13] X. Zhang, Phys. Rev. **D 51**, 5309 (1995); J. Berger, A. Blotz, H.-C. Kim and K Goeke, Phys. Rev. **D 54**, 3598 (1996).
- [14] E. Malkawi and T. Tait, Phys. Rev. **D 54**, 5758 (1996).
- [15] A.D. Martin, R.G. Roberts and W.J. Stirling, Phys. Rev. **D 50**, 6734 (1994).
- [16] S. Cortese, R. Petronzio, Phys. Lett. **B 253**, 494 (1991); Douglas O. Carlson and C.P. Yuan, in proc. of the Workshop on Physics of the Top Quark, *Particle Theory and Phenomenology*, ed. by K. Lassila *et al.* (World Scientific, Singapore, 1996), p. 172; T. Stelzer, S. Willenbrock, Phys. Lett. **B 357**, 125 (1995); A.P. Heinson, A.S. Belyaev, E.E. Boos, Phys. Rev. **D 56**, 3114 (1997); T. Stelzer, Z. Sullivan, S. Willenbrock, Phys. Rev. **D 56**, 5919 (1997).
- [17] F.A. Berends, H. Kuijf, B. Tausk and W.T. Giele, Nucl. Phys. **B 357**, 32 (1991).
- [18] M. Hosch, *Flavor-changing chromo-magnetic moments: a monte carlo study of the top quark*, Ph.D. thesis, Iowa State University, 1998.

Table 1: Optimized cuts for the discovery of $\frac{\kappa_f}{\Lambda}$ with single top quark production for several collider options.

	$M_{bW,min}$	$M_{bW,max}$	$p_{Tb,min}$	$\Delta R_{jj,min}$	$\Delta R_{jl,min}$
Tevatron Run 1	150 GeV	200 GeV	35 GeV	1.0	0.4
Tevatron Run 2	150 GeV	200 GeV	35 GeV	1.5	1.5
Tevatron Run 3	150 GeV	200 GeV	35 GeV	1.5	1.5
LHC	145 GeV	205 GeV	35 GeV	1.5	1.0

Table 2: Cross sections in fb for the individual signal (with $\kappa_f/\Lambda = 0.2 \text{ TeV}^{-1}$) and background channels after the cuts in Eqs. (4)–(6) and in Table 1 are employed. Cross sections after b -tagging are shown in parentheses. The signal values scale quadratically for $\kappa_f/\Lambda \lesssim 0.2 \text{ TeV}^{-1}$.

$\bar{t}cg$	Run 1		Runs 2 & 3		LHC	
$q\bar{q} \rightarrow t\bar{c}$	23	(8)	15	(9)	200	(120)
$gg \rightarrow t\bar{c}$	87	(32)	76	(45)	15200	(9090)
$cq \rightarrow tq$	56	(20)	52	(31)	4087	(2450)
$cg \rightarrow tg$	130	(47)	115	(69)	21150	(12650)
Total	296	(107)	258	(154)	40460	(24310)
$\bar{t}ug$	Run 1		Runs 2 & 3		LHC	
$q\bar{q} \rightarrow t\bar{u}$	23	(8)	15	(9)	200	(120)
$gg \rightarrow t\bar{u}$	87	(32)	76	(45)	15200	(9090)
$uq \rightarrow tq$	1005	(365)	832	(498)	24760	(14810)
$ug \rightarrow tg$	3025	(1097)	2381	(1424)	146200	(87430)
Total	4140	(1502)	3304	(1976)	186360	(111450)
SM background	Run 1		Runs 2 & 3		LHC	
$bq \rightarrow tq$	156	(57)	149	(89)	14570	(8710)
$q\bar{q} \rightarrow t\bar{b}$	42	(19)	29	(14)	390	(190)
$Wb\bar{b}$	62	(29)	13	(6)	160	(80)
Wjj	7616	(151)	2270	(45)	97370	(1930)
Total	7876	(256)	2461	(154)	112490	(10910)

Table 3: The discovery limits on κ_c/Λ and κ_u/Λ for each of the collider options discussed in the text. In both the charm and up quark cases, we assumed that the coupling of the other type did not exist.

	Tevatron			
	Run 1	Run 2	Run 3	LHC
E_{cm} (TeV)	1.8	2.0	2.0	14.0
\mathcal{L} (fb ⁻¹)	.1	2	30	10
κ_c/Λ (TeV ⁻¹)	.31	.092	.046	.013
κ_u/Λ (TeV ⁻¹)	.082	.026	.013	.0061

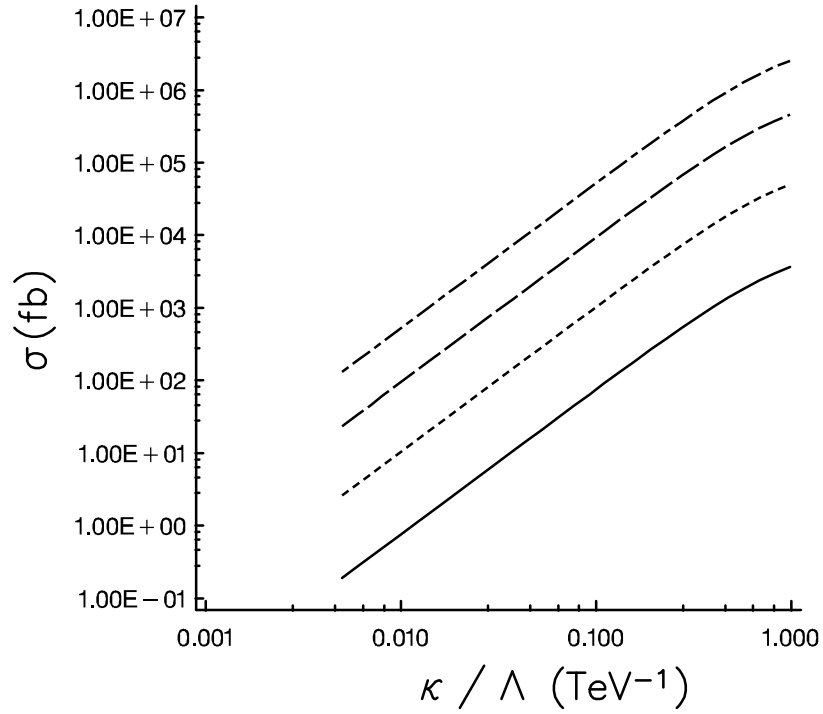


Figure 1: Cross sections for single top-quark production $pp(\bar{p}) \rightarrow tj$ versus κ_f/Λ at the Tevatron and LHC. The solid and short dashed lines are for the $\bar{t}cg$ and $\bar{t}ug$ coupling at the Tevatron, respectively. The long dashed and dash-dotted lines are at the LHC.

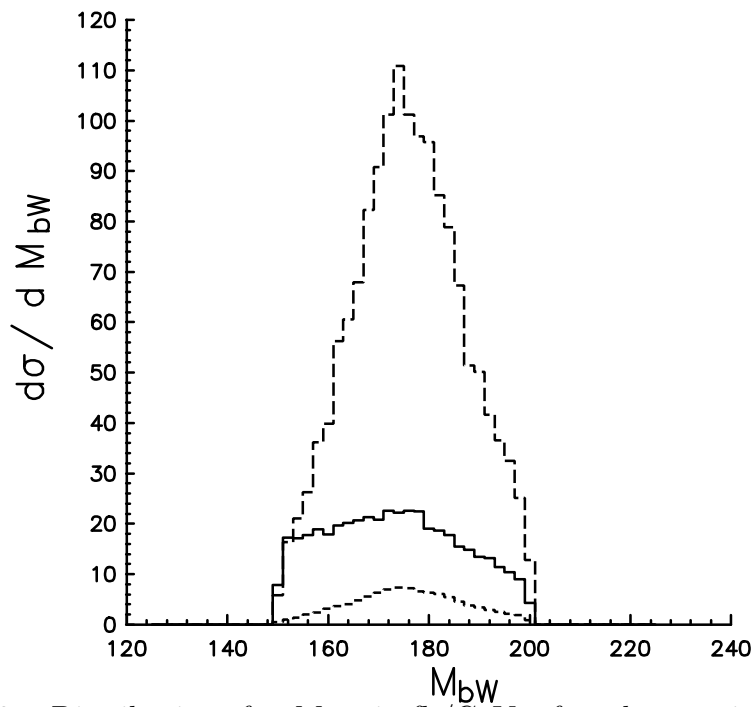


Figure 2: Distributions for M_{bW} , in fb/GeV, after the cuts in Eqs. (4)–(6) and (12)–(14) and b -tagging at the Tevatron Run 1. The solid line represents the sum of all of the background processes, the long dashed line is the sum of the up-quark signal processes, and the short dashed line is the sum of the charm-quark signal processes, with $\kappa_f/\Lambda = 0.2 \text{ TeV}^{-1}$.

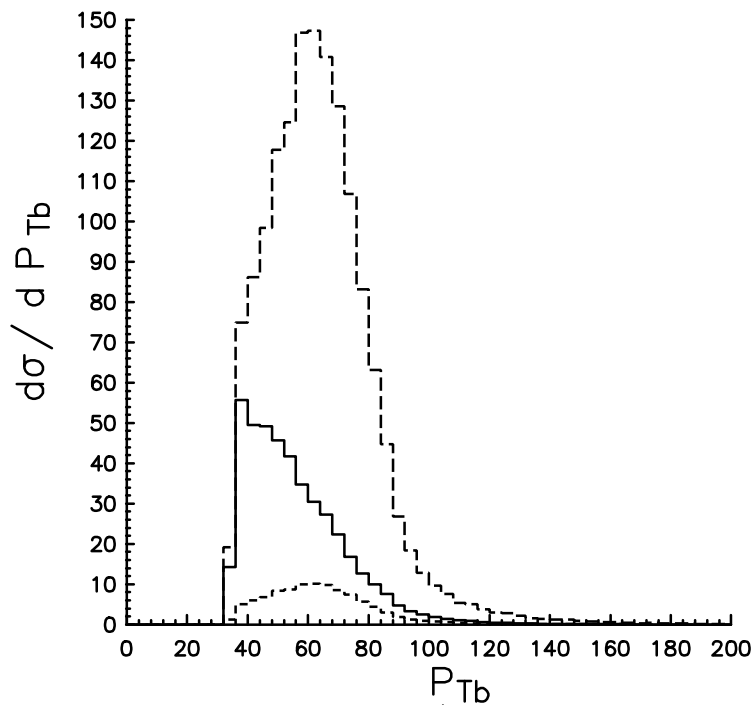


Figure 3: Distributions for p_{Tb} , in fb/GeV, after the cuts in Eqs. (4)–(6) and (12)–(14) and b -tagging at the Tevatron Run 1. The solid line represents the sum of all of the background processes, the long dashed line is the sum of the up-quark signal processes, and the short dashed line is the sum of the charm-quark signal processes, with $\kappa_f/\Lambda = 0.2 \text{ TeV}^{-1}$.

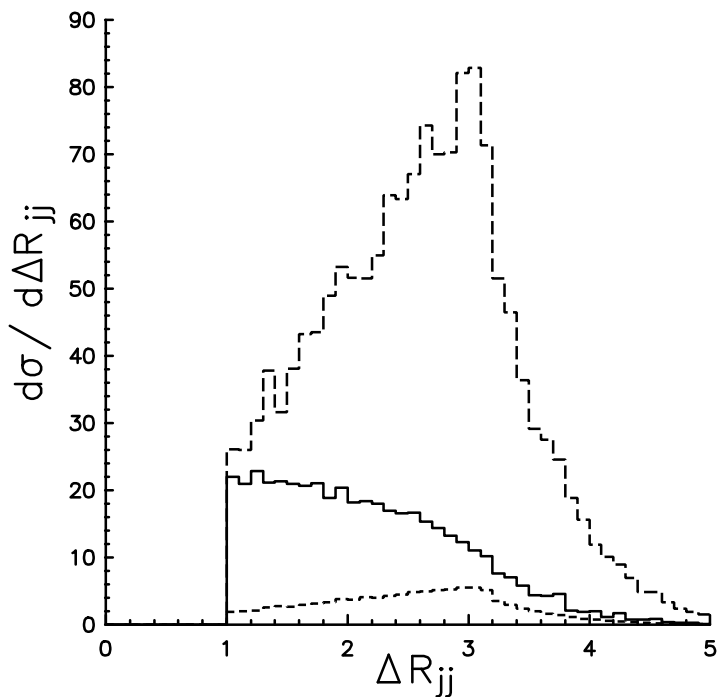


Figure 4: Distributions for ΔR_{jj} , in fb per unit ΔR_{jj} , after the cuts in Eqs. (4)–(6) and (12)–(14) and b -tagging at the Tevatron Run 1. The solid line represents the sum of all of the background processes, the long dashed line is the sum of the up-quark signal processes, and the short dashed line is the sum of the charm-quark signal processes, with $\kappa_f/\Lambda = 0.2 \text{ TeV}^{-1}$.

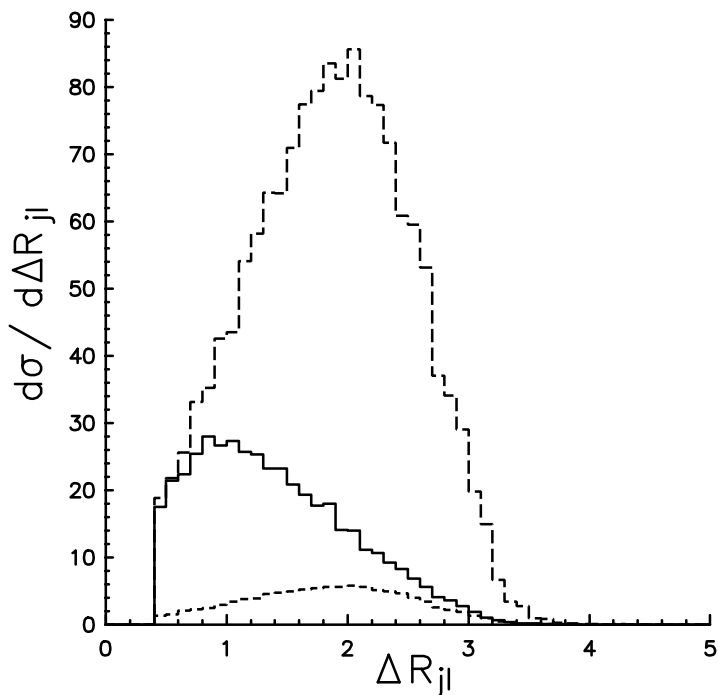


Figure 5: Distributions for ΔR_{jl} , in fb per unit ΔR_{jl} , after the cuts in Eqs. (4)–(6) and (12)–(14) and b -tagging at the Tevatron Run 1. The solid line represents the sum of all of the background processes, the long dashed line is the sum of the up-quark signal processes, and the short dashed line is the sum of the charm-quark signal processes, with $\kappa_f/\Lambda = 0.2 \text{ TeV}^{-1}$.

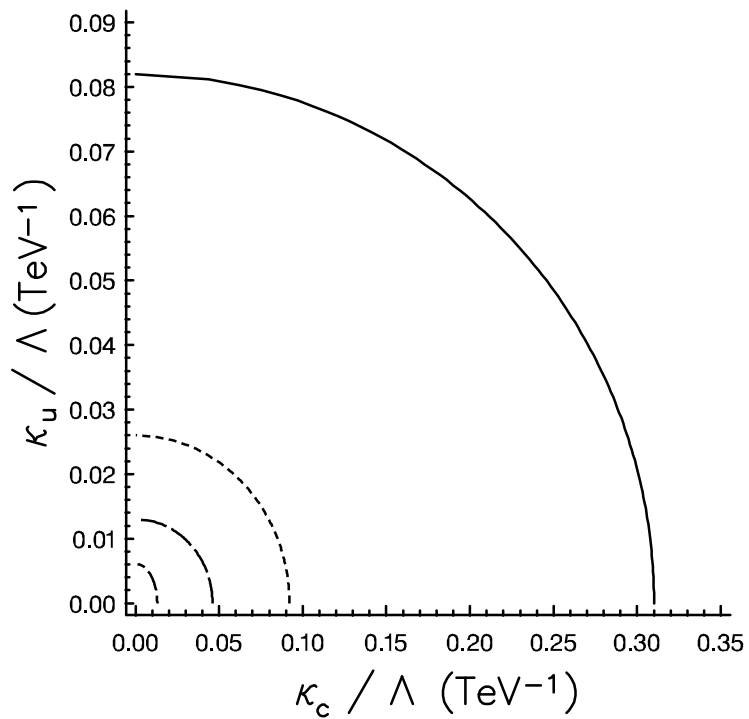


Figure 6: Discovery limits for κ_c/Λ versus κ_u/Λ for each of the collider options considered. The solid, short dashed, and long dashed lines are at Runs 1, 2, and 3 at the Tevatron respectively. The dash-dotted line is at the LHC.